BioGecko

Vol 12 Issue 02 2023

ISSN NO: 2230-5807

BRAIN TUMOR SEGMENTATION AND GRADING FROM MRI IMAGES USING DEEP NEURAL ARCHITECTURES

Para Rajesh[1],Dr. A.Punitha[2],P.Chandra Sekhar Reddy[3]

[1]Research Scholar, Department of Computer Science and Engg, Faculty of Engineering and Technology, Annamalai University, Chidambaram, Annamalai Nagar – 608002, Tamil Nadu, India.
pprr21@gmail.com

[2]Department of Computer Science and Engg,, Faculty of Engineering and Technology, Annamalai University, Chidambaram, Annamalai Nagar – 608002, Tamil Nadu, India.
12charuka17@gmail.com

[3]Computer Science and Engg. Dept., Gokaraju Rangaraju Institute of Engineering and Technology, Hyderabad-500090, Telangana, India.
pchandureddy@yahoo.com

ABSTRACT

Brain tumor segmentation is the process of distinguishing the tumor region from the normal brain tissue region; in conventional diagnosis process this segmentation or localization shall aid for prognosis and plan treatment or surgical process. In reality the uneven structure and hazy limits of tumors causes greater challenges and issues. Also the segmentation can be considered as the process of localization of tumor present in the MRI images. Ascancerous region vary in size and position, accurate and efficient segmentation of tumors remains a difficult undertaking. They frequently have complicated, non-rigid shapes with a variety of appearance qualities. Additionally, the tumors exhibit significant variations in appearance from patient to patient, as a result there is a need to add physical information about the tumor to enhance the accuracy of the segmentation process.The segmentation process becomes more complex when the tumor region overlap with normal brain tissues, particularly in tumor borders.The efficient deep neural architectures are employed in this study. This work shall focus on the design and development of a deep neural network based segmentation usingLinkNET, and U-NET (with EfficientNet based encoder), fully convolutional neural network. This localization task shall help the physician to decide on the further prognosis and treatment process. Further by analyzing the segmented tumor region, tumor categorization can be done by using a classification model.

Keywords: deep neural architecture, U-NET,EfficientNet brain tumor, MRI images, segmentation, grading, classification model, tumor categorization.

1. INTRODUCTION

A group of aberrant cells that proliferate uncontrollably in the brain are what make up a brain tumor. There are many different forms of brain tumors that can be categorized into two groups: benign and malignant. Benign tumors are often easier to remove surgically than malignancies because they are less belligerent, develop more gradually, and persistsecluded from the neighboring normal brain tissues. It might be challenging to distinguish malignant brain tumors from the nearby normal tissues. As a result, it might be challenging to completely remove them without causing harm to the surrounding brain regions. Malignant brain tumors have been affecting more people over the past few decades. According to the International

Association of Cancer Registries, brain tumors cause about 24,000 deaths each year (IARC). According to a research, the market for brain tumor treatment is anticipated to develop at a growth rate of 1.11 percent annually until 2030. If the predictions come true, brain tumors may overtake leukemia as the second most frequent malignancy by 2030, according to medical experts. According to estimates, 40,000–50,000 persons in India receive a brain tumor diagnosis each year. Children make up roughly 20% of these.

Magnetic Resonance provides images with high resolution and excellent contrast across tissues, MRI is a noninvasive medical imaging technique that is frequently utilized in daily clinical practice. For a more precise prognosis and providing healthcare service, MRI offers abundant information regarding the structure, volume, and position of tumors [1, 2]. As a result, MRI images are mostly used in studies on the medical prognosis and brain tumors localization. Weighted images, often known as MRI slices, include T1-weighted, T2-weighted, proton-density weighted, and fluid-attenuated inversion recovery (FLAIR). T1-weighted contrast stretched images and FLAIR are frequently utilized for brain tumor analysis since it makes cancerous region hyperintense. T1-weighted images provide a better visualizationof cancerous and healthy tissuesby exploiting the high contrast between grey and white matter [3].

It is essential and difficult to accurately segment brain tumors using MRI images for prognosis and treatment planning. The process of finding one or more sub-regions defining the region of interest is known as image segmentation and is a current focus of research in the area of biomedical imaging. A variety of algorithms, such as threshold-based approaches [4, 5], region-based methods [6, 7], deformable methods [8, 9], classification methods [10, 11], and deep learning [12, 13], were proposed in the literature to detect tumors in the human brain. Brain cancers are frequently detected, and brain tumor segmentation involves separating the malignant zone from healthy brain regions. However, since tumors can differ in size and position, accurate and efficient segmentation of tumors continues to be a difficult process. They frequently have complicated, non-rigid shapes with a variety of appearance qualities. Additionally, they exhibit significant patient-to-patient variability in appearances [14]. They also exhibit intensities overlapping with normal brain tissues, particularly in the borders of the tumors[44][45].

This work shall focus on segmentation of the tumor region by using a fully convolutional neural network modelLinkNET. The majority of the currently used methods for deep learning based localization of tumors use an encoder-decoder pair as the foundation of the network design, which were inspired by auto-encoders [3], [15]. The segmentation process begins with the encoder encoding data into feature space, which the decoder then projects into spatial categorization. The pooling indices or complete convolution are typically used to recover spatial information that was erodedbecause of the pooling/ convolution operation during the encoding process. By using the fully convolutional neural architectures the model the segmentation accuracy is increased along with a significant reduction in processing time by diverting spatial information and going straight from the encoding block to the associated decoding block. In this approach, information that would have been lost at each encoder level is saved, saving time and resources that would have been used to re-learn the lost knowledge.

2. LITERATURE SURVEY

A most difficult task in the process of analysis of medical images is brain tumor segmentation. To accurately delineate the regions of brain tumors is the focus of cancer analysis. Deep learning techniques have recently demonstrated better results in resolving a number of issues in the field of machine vision, including semantic segmentation, object detection, and image categorization. Many deep learning-based techniques were used to segment brain tumors with encouraging success. The strategies for segmenting brain tumors using deep learning that have recently been developed are covered in detail in this section.

Both the prognosis and treatment of Gliomas, a most commonly occurring type of brain tumor that arises from glial cells, actively involve image segmentation. For instance, a precise glioma segmentation mask may aid in the planning of the operation, postoperative surveillance, and the improvement of the survival rate [16, 17]. The task of brain tumordetection/segmentation can be described as follows in order to measure the

result of image segmentation: The model attempts to segment the cancerous region from the healthy tissues given an input image from one or more imaging modalities, for example, several MRI sequences, by categorizing each pixel present in the raw image into a category oftumor. The segmentation map of the related input is then returned by the system. Data imbalance has long been a problem in bio-medical image processing. Researchers experiment with a variety of strategies to effectively address the imbalance problem, including an ensemble techniqueor cascaded network [18], multiple learning tasks [18], and tailored error functions [20]. Making the most of multi-information modalities is another option. Recent studies mainly addressed modality fusion [21] and modality missing [22].

There are several unresolved problems in the detection of brain tumors through MR image analysis. When creating efficient segmentation models, two principles should be kept in mind. Through the extension of the receptive field [23], attention layer [24], fusion of featuremaps [25], and other forms, one is to extract higher semantics and locate the object of interest. The alternative is to improve the training and inference while reducing the number of network parameters, which will save computational time and resources [26]. The migration from a single channel network to a multi-channel network, from a network with densely connected layers to a fully-convolutional layers, and from a simple network to a deep cascaded network are the key ways in which the design of the network architecture is reflected. The goal is to further the network's depth, improve the network's capacity for feature learning, and achieve more accurate segmentation [41].

Many techniques for accurately segmenting brain tumors based on creating efficient models of neural networks, stabilized training, and learning informative, discriminative characteristics. Early attempts at design stacked convolutional blocks to gradually improve network depth, imitating well-known networks like AlexNet [27]. Convolutional layers made up of many blocks with a kernel size usually larger than 5 were layered in early research works like [28, 29], pooling and activation functions together. It is possible to extractcoarse to fine details with more number of learnable parameters to be taught by combining blocks with a convolution kernel of larger size. Other research projects, like [30], adopted the strategy used by VGG [31] to construct convolutional layers using a small-sized kernel (usually three) as the fundamental building block. Additional studies followed stacking of hybrid blocks [32] having different size of kernels, where kernels of larger sizeare capable of finding global features such as position and volume with a large receptive field and kernels of smaller size typically extract local features such as boundary and textural pattern with a small receptive field [38][40].

Gradient vanishing and explosion problems were resolved as the network becoming deeper by increasing the number of stacked layers. Early brain tumor segmentation algorithms like [33] and [34] adopted ResNet [35] and added residual connection into module design for stabilizing model training and achieve better segmentation. The problem of gradient explosion and vanishing can be solved by passing the input of the convolution block to its output through a residual connection. This prevents degradation and converges more quickly and accurately. The current standard procedure for designing models and intricate network structures employs a residual connection. The authors of the works listed below [36] enlarged residual connection to dense connection in accordance with DenseNet [37]. Even while a dense connection design appears to be more suitable for gradient back-propagation, the intricate close connection topology may need several memory operations while the network is being trained.The segmentation of tumor region in the MRI using various deep learning techniques is a difficult task. Due to deep learning's strong feature learning capabilities, automated brain tumor segmentation has various advantages [42]This work shall implement the two deep segmentation model;LinkNET(U-NET with EfficientNet based encoder) and compare their performance[43].

3. MATERIALS AND METHOD

3.1 Dataset

Benchmark dataset, BR35H, containing brain tumor MRIs is used for training the segmentation model which contains a total of 804 MRI images (train-501; validation-202; and test-101). The dataset were used to train

the U-NET model. Images of different category of tumors (benign, malignant, and pituitary) are available in the dataset.

3.2 Pre-Processing

The quality of the scanned photographs was extremely variable because they were obtained using various scanners and acquisition conditions. The goal of our work was to improve the image quality of the low-quality MRI by normalizing the histogram of the low-quality MRI to the histogram of the high-quality MRI. As a result, it is essential to evaluate the photographs' quality first. For the purpose of evaluating MRI quality, numerous strategies have been put forth [38]. In order to evaluate the quality of the image, we will utilize a histogram as our intensity normalization method tries to normalize histograms. The noise estimation index $\hat{\sigma}_n$ can be expressed mathematically as;

$$\hat{\sigma}_n = \text{mode}\{\text{M(x)}\}$$

Where $\text{mode}\{\text{M(x)}\}$ represents the mode of the distribution. The generated index allows for a direct evaluation of MRI quality. A lower estimation index value denotes a higher level of image quality.

- **Normalization using Histogram**

Let$\boldsymbol{I}(\boldsymbol{x})$represents the MRI of human brain where $x \in [0, N] \times [0, M] \times [0, L] \subset \mathbb{N}^3$ where N, M, L is the dimensions of I, and B denotes the binary mask of the tumor image ($B \subset I$). This paper employs kernel density estimation technique for normalization which estimate the probability density function of the intensities of I over the brain mask B. The KDE of the probability density function is estimated as follows;

$$\hat{\boldsymbol{p}}(\boldsymbol{x}) = \frac{\mathbf{1}}{\boldsymbol{N.M.L.\delta}} \sum_{\boldsymbol{i=1}}^{\boldsymbol{N.M.L}} \boldsymbol{K}\left(\frac{\boldsymbol{x} - \boldsymbol{x_i}}{\boldsymbol{\delta}}\right)$$

where$x$ is a pixel intensity value, K is the kernel function non-negative which integrates to 1, and δ is a smoothing parameter used for scaling the kernel function. A gaussian kernel is used and the δ parameter is set to a value of 80. With the use of a combinatorial optimization method, we can more reliably select the mode related to the White Matter using the kernel density estimate's smooth form of the histogram. The entire image is then normalized using the discovered White Matter peak p. The result of the normalization is presented in Fig. 1

$$I_{kde}(x) = \frac{c.I(x)}{p}$$

Where $c \in \mathbb{R}_{>0}$is a constant and the value of$c$is set to 1 in the experiments.

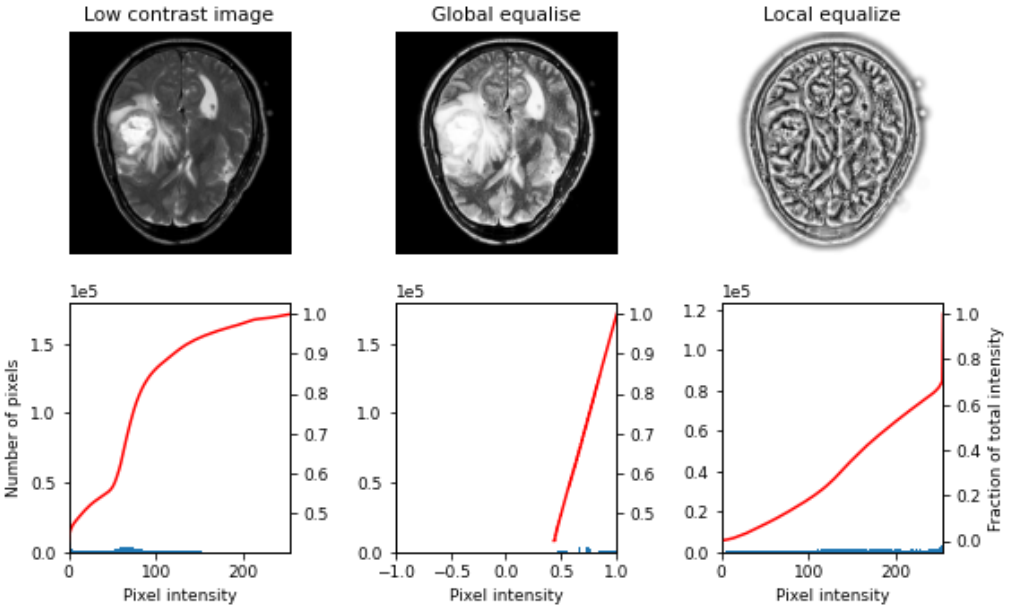

Fig. 1 Result of Histogram Equalization

3.3 Architecture ofU-NET with EfficientNet Encoder

UNet is a fully convolutional neural network with a symmetric U shape that was initially created for biomedical picture segmentation. The encoder-decoder module typically comprises of a CNN-based encoder that extracts the features from the original image. To capture fine details in the image, it down-samples the image gradually and lowers the feature map resolution. To produce the final feature map, these CNN architectures often gradually decrease the input resolution of the image. Reconstructing the segmentation map of the original image's size from the smaller feature map is difficult. In order to retrieve spatial information, the decoder module consists of a number of layers that up-sample the feature map of the encoder. In a traditional UNet, the expansion path and the contraction path are almost symmetrical. In contrast to the traditional set of convolution layers, it is suggested using EfficientNet as an encoder in the contracting path. The decoder module resembles the first-generation UNET (presented in Fig. 3).

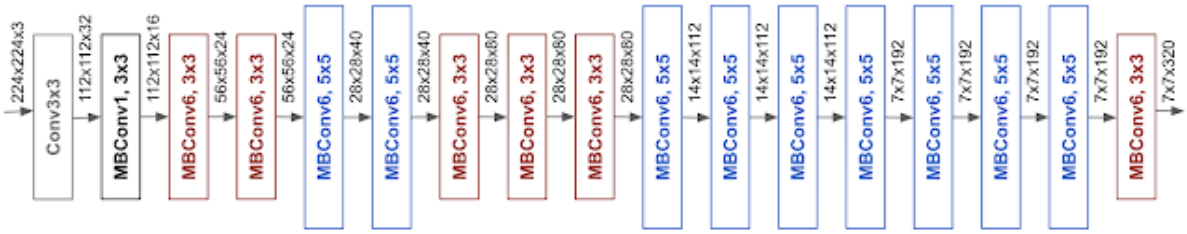

Fig. 2 Architecture of EfficientNet

Figure 2 shows the encoder's block architecture in detail. EfficientNet is a cutting-edge model scaling technique that uses a straightforward but incredibly powerful compound coefficient to scale up CNNs in a more organized way. This architecture evenly scales every dimension with a specific set of scaling coefficients, in contrast to conventional techniques that arbitrary scale network dimensions like width, depth, and resolution. The baseline network is crucial to the success of model scaling. Therefore, a new baseline network is created by performing a neural architecture search using the AutoML MNAS framework, which maximizes both accuracy and efficiency, to further increase performance (FLOPS). Similar to MobileNetV2 and MnasNet, this architecture utilizes mobile inverted bottleneck convolution (MBConv), however it is a little bigger because of a bigger FLOP budget.The last logit of the encoder's feature map must first be

bilinearlyupsampled by a factor of two before being concatenated with the feature map from the encoder with the same spatial resolution. 3x3 convolution layers are added after that, and then another upsampling by a factor of two follows. The procedure is repeated until the segmentation map is recreated with a size equal to the input image. Unlike the original UNet, the suggested architecture is asymmetrical. In this case, the expansion path is shallower than the contraction path. The method performs better overall as anefficient CNN encoder, such EfficientNet, is used.

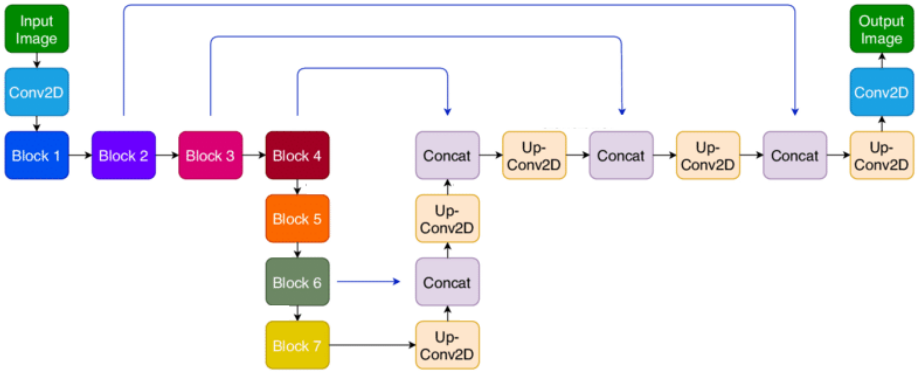

Fig. 3 Schematic view of connections in Encoder-Decoder blocks of U-NET [39]

3.4 Architecture of LinkNET

In the LinkNET architecture, a novel connection has been added between the encoder and decoder block to achieve precise instance level prediction without slowing down the network's processing time. The pooling indices or complete convolution are typically used to recover spatial information that was lost in the encoder due to pooling or strided convolution. By using this architecture, the information that would have been lost at each level of encoding is maintained, saving time and resources that would have been used to re-learn the lost knowledge. The architecture of the LinkNET model is presented in Fig. 4. Conv in this context refers to a convolution, and full-conv to a full convolution. Furthermore, strided convolution is used to accomplish /2 denotes down-sampling by a factor of 2, and 2 denotes up-sampling by a factor of 2. Between each convolutional layer and ReLU non-linearity, we employ batch normalization. The encoder is located in the left part of the network, and the decoder is located on the right. Beginning with the first block, the encoder performs convolution on the input picture using a kernel of size 77 and a stride of 2. Additionally, this block conducts spatial max-pooling in a 3 by 3 area with a 2 stride. The remaining blocks that make up the later part of the encoder are referred to as encoder-blocks.

The uniqueness of the architecture is seen in the connections between each encoder and decoder. Significant spatial information is lost as a consequence of the encoder's successive downsampling procedures. It is challenging to restore this lost data using only the encoder's output that has been downscaled. The input of each encoder layer is also passed to the output of its matching decoder in this research based on [15]. The goal is to retrieve lost spatial data that the decoder and its upsampling processes can employ. Additionally, the decoder can use fewer parameters because it is sharing the information that the encoder learned at each layer. When compared to the current state-of-the-art segmentation networks, this leads to an overall more efficient network and, consequently, real-time operation.

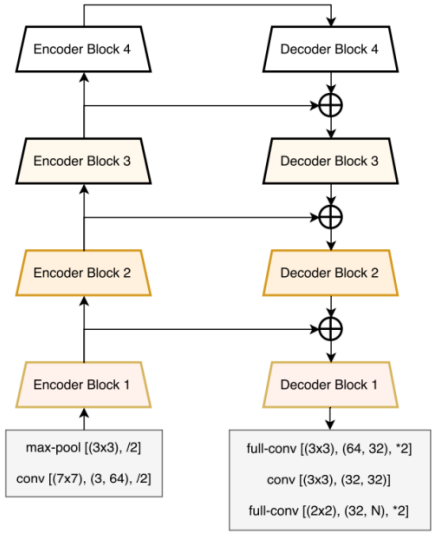

Fig.4LinkNET Architecture [15]

3.5 Performance Metrics

The Intersection-Over-Union (IoU) metric also known as Jaccard Index, is a commonly applied metrics in pixel-wise segmentation. The IoU is estimated by finding the ratio between the area of union between the generated mask by the model and the ground truth by the overlapped-region between the predicted and ground truth mask. The value of IoU metric can range between 0 and 1, with 0 representing complete overlap and 1 representingzero overlap. The Dice Coefficient is estimated by finding the ratio between the number of pixels in both by the area of overlap multiplied by two. The Jaccard Index and the Dices' coefficient are quite similar. They are linearly related, thus if one metric proves a model A is superior to model B at segmentation, the other metric will also reflect the same.IoU can be expressed mathematically as; $J(A,B) = \frac{|A \cap B|}{|A \cup B|} = \frac{|A \cap B|}{|A|+|B|-|A \cap B|}$ where A and B denotes the segmented mask and the ground truth mask. Similarly the Dice's Coefficient also known as F1 score can be expressed mathematically as $\frac{2|A \cap B|}{|A|+|B|}$.

4. RESULTS AND ANALYSIS

The segmentation models were trained on images of size 300×300 (original images of size 630x630 were resized to 300x300), with a batch size of 16 and for 200 epochs. To analyze the performance of the different fully convolutional neural architectures the U-NET, U-NET+EfficientNET, and LinkNET architectures were considered. The encoder used in U-NET+EfficientNETwas initialized with pre-trained weights of EfficientNetB7 trained on ImageNetdataset. Image augmentation techniques were adopted to prevent the model from overfitting. Pre-processed images were augmented and the models were configured with ADAM optimizer and learning rate of 0.001 during the training process.

The loss function is based on the sum of IoU and binary cross-entropy. The performance of the models are evaluated based on the mean Intersection over Union (mIoU). IoUvaluesare computed as follows; $IoU = \frac{TP}{TP+FP+FN}$.The LinkNET architecture is less difficult than competing architectures like U-NET with EfficientNET encoder because ResNet-50 has a limited number of layers with a smaller number of trainable parameters. In order to extract useful multi-scale features with fewer parameters and a higher number of layers, the encoder leverages residual connections between the layers.

Table 1. Segmentation Results of LinkNET model on test images

Raw Image	Ground Truth Mask	Segmented Mask

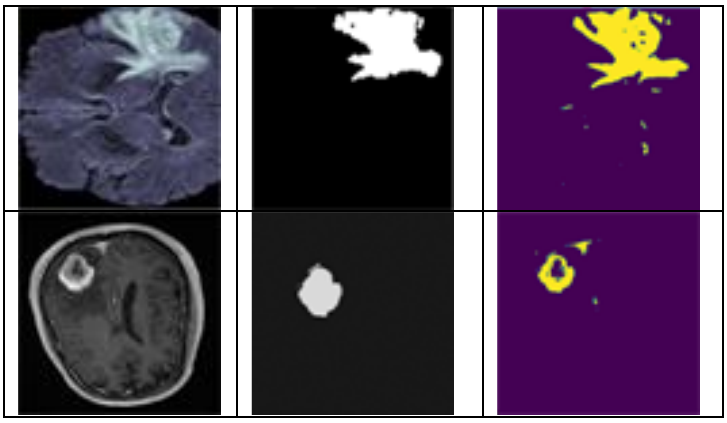

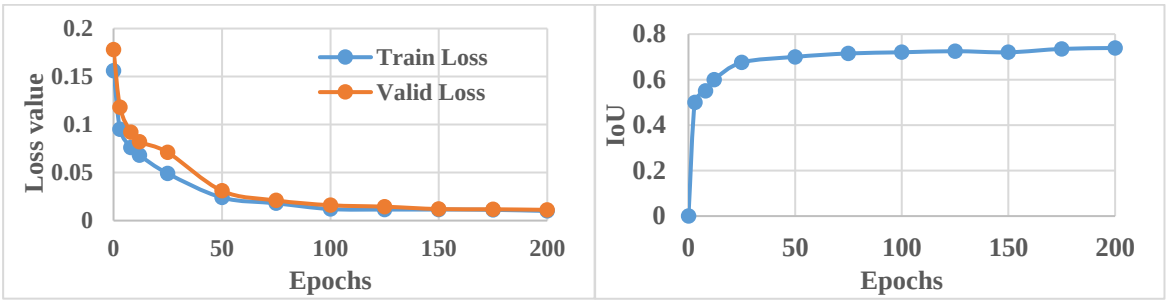

Fig.5 Loss value and IoU Graph of U-Net with EfficientNet-B7

Fig. 5 presents the loss value and JI score recorded during the training process of segmentation models and the prediction of tumor mask for few test cases by the trained LinkNET model was were presented in Table 1. The LinkNET model showed better performance when compared to U-NET based segmentation models where the Dice's coefficient of the LinkNET model was 0.9876 with an accuracy of 98.04%.

Table 2. Performance analysis of segmentation models

Model	Loss Function	Dice's Coefficient	Jaccard Index	Accuracy	Precision	Recall	Specificity
LinkNET with ResNET50 Encoder	0.009236	0.9876	0.7392	0.9892	0.9804	0.9824	0.9923
U-NET+EffNetB7	0.009632	0.9815	0.7328	0.9854	0.9794	0.9798	0.9896
U-NET	0.010018	0.9626	0.7264	0.9618	0.9645	0.9638	0.9818

CONCLUSION

The complexity of MRI brain imaging may make it difficult to segment brain tumors, but its goals to predict malignancies by using artificial intelligence models make this work important. The recommended system uses Link-Net and U-NET with a number of pre-trained models as an encoder architecture to extract discriminating features between the brain normal tissue region and the tumor/ cancerous region for automatic localization/ segmentation of brain tumors. They make the imaging and segmentation of brain tumors easier and faster. Performance-wise, the ResNet encoder-based LinkNET design showed better performance when compared to U-NET based architectures. The LinkNET model achieved an accuracy of 0.9892 with a Dice's

coefficient of 0.9876 and precision of 0.9804. The limitations of the 2D segmentation algorithm prevent it from fully utilizing MRI data; as a result, the architecture loses semantics and local properties between slices. In order to increase segmentation accuracy, the work could be broadened in the future by creating more potent patch extraction methods. However, this study can be expanded to include the development of models to be trained on 3D images in order to uncover efficient ways to extract 3D slices. So far, we have only introduced the usage of 2D slices of MRI for extraction and training.

REFERENCES

1. J. Liu, M. Li, J. Wang, F. Wu, T. Liu, and Y. Pan, "A survey of MRI-based brain tumor segmentation methods," Tsinghua Science and Technology, vol. 19, no. 6, pp. 578–595, 2014.
2. S. Bauer, R. Wiest, L. P. Nolte, and M. Reyes, "A survey of MRI based medical image analysis for brain tumor studies," Physics in Medicine & Biology, vol. 58, no. 13, pp. 97–129, 2013.
3. G. Helms, K. Kallenberg, and P. Dechent, "Contrast-driven approach to intracranial segmentation using a combination of T2- and T1-weighted 3D MRI data sets," Journal of Magnetic Resonance Imaging, vol. 24, no. 4, pp. 790–795, 2006.
4. P. Gibbs, D. Buckley, S. Blackb, and A. Horsman, "Tumour determination from MR images by morphological segmentation," Physics in Medicine & Biology, vol. 41, no. 11, pp. 2437–2446, 1996.
5. A. Stadlbauer, E. Moser, S. Gruber et al., "Improved delineation of brain tumors: An automated method for segmentation based on pathologic changes of 1H-MRSI metabolites in gliomas," NeuroImage, vol. 23, no. 2, pp. 454–461, 2004.
6. M. R. Kaus, S. K. Warfield, A. Nabavi, P. M. Black, F. A. Jolesz, and R. Kikinis, "Automated segmentation of MR images of brain tumors," Radiology, vol. 218, no. 2, pp. 586–591, 2001.
7. W. Deng, W. Xiao, H. Deng, and J. Liu, "MRI brain tumor segmentation with region growing method based on the gradients and variances along and inside of the boundary curve," in Proceedings of the 3rd International Conference on BioMedical Engineering and Informatics, BMEI 2010, pp. 393–396, China, October 2010.
8. S. Taheri, S. H. Ong, and V. F. H. Chong, "Level-set segmentation of brain tumors using a threshold-based speed function," Image and Vision Computing, vol. 28, no. 1, pp. 26–37, 2010.
9. A. M. Hasan, F. Meziane, R. Aspin, and H. A. Jalab, "Segmentation of brain tumors in {MRI} images using three-dimensional active contour without edge," Symmetry, vol. 8, no. 11, Art. 132, 21 pages, 2016.
10. L. M. Fletcher-Heath, L. O. Hall, D. B. Goldgof, and F. R. Murtagh, "Automatic segmentation of non-enhancing brain tumors in magnetic resonance images," Artificial Intelligence in Medicine, vol. 21, no. 1-3, pp. 43–63, 2001.
11. A. Veloz, S. Chabert, R. Salas, A. Orellana, and J. Vielma, "Fuzzy spatial growing for glioblastomamultiforme segmentation on brain magnetic resonance imaging," LNCS, vol. 4756, pp. 861–870, 2008.
12. M. Havaei, A. Davy, D. Warde-Farley et al., "Brain tumor segmentation with Deep Neural Networks," Medical Image Analysis, vol. 35, pp. 18–31, 2017.
13. A. Işin, C. Direkoğlu, and M. Şah, "Review of mri-based brain tumor image segmentation using deep learning methods," Procedia Computer Science, vol. 102, pp. 317–324, 2016.
14. N. Gordillo, E. Montseny, and P. Sobrevilla, "State of the art survey on MRI brain tumor segmentation," *Magnetic Resonance Imaging*, vol. 31, no. 8, pp. 1426–1438, 2013.
15. Chaurasia, Abhishek, and Eugenio Culurciello. "Linknet: Exploiting encoder representations for efficient semantic segmentation." *2017 IEEE visual communications and image processing (VCIP)*. IEEE, 2017.

16. Baid U, Ghodasara S, Mohan S, Bilello M, Calabrese E, Colak E, Farahani K, Kalpathy-Cramer J, Kitamura FC, Pati S, et al. (2021) Thersna-asnr-miccai brats 2021 benchmark on brain tumor segmentation and radiogenomic classification.
17. Bakas S, Akbari H, Sotiras A, Bilello M, Rozycki M, Kirby JS, Freymann JB, Farahani K, Davatzikos C (2017) Advancing the cancer genome atlas gliomamri collections with expert segmentation labels and radiomic features. Sci Data 4(1):1–13
18. Jiang Z, Ding C, Liu M, Tao D (2019) Two-stage cascaded u-net: 1st place solution to brats challenge 2019 segmentation task. In: International MICCAI Brainlesion Workshop, pp. 231–241. Springer
19. Myronenko A (2018) 3d mri brain tumor segmentation using autoencoder regularization. In: International MICCAI Brainlesion Workshop, pp. 311–320. Springer
20. Sudre CH, Li W, Vercauteren T, Ourselin S, Cardoso MJ (2017) Generalised dice overlap as a deep learning loss function for highly unbalanced segmentations. In: Deep learning in medical image analysis and multimodal learning for clinical decision support, pp. 240–248. Springer
21. Zhang D, Huang G, Zhang Q, Han J, Han J, Yu Y (2021) Cross-modality deep feature learning for brain tumor segmentation. Pattern Recogn 110:107562
22. Zhou T, Canu S, Vera P, Ruan S (2021) Latent correlation representation learning for brain tumor segmentation with missing mri modalities. IEEE Trans Imag Process 30:4263–4274.
23. Li X, Zhang X, Luo Z (2017) Brain tumor segmentation via 3d fully dilated convolutional networks. In: Multimodal Brain Tumor Segmentation Benchmark, Brain-lesion Workshop, MICCAI, vol. 9, p. 2017
24. Islam M, Vibashan V, Jose VJM, Wijethilake N, Utkarsh U, Ren H (2019) Brain tumor segmentation and survival prediction using 3d attention unet. In: International MICCAI Brainlesion Workshop, pp. 262–272. Springer
25. Liu C, Ding W, Li L, Zhang Z, Pei C, Huang L, Zhuang X (2020) Brain tumor segmentation network using attention-based fusion and spatial relationship constraint. arXiv preprint arXiv:2010.15647
26. Andermatt S, Pezold S, Cattin P (2017) Multi-dimensional gated recurrent units for brain tumor segmentation. In: International MICCAI BraTS Challenge. Pre-Conference Proceedings, pp. 15–19
27. Krizhevsky A, Sutskever I, Hinton GE (2012) Imagenet classification with deep convolutional neural networks. Adv Neural Inf Process Syst 25:1097–1105
28. Dvořák P, Menze B (2015) Local structure prediction with convolutional neural networks for multimodal brain tumor segmentation. In: International MICCAI workshop on medical computer vision, pp. 59–71. Springer
29. Rao V, Sarabi MS, Jaiswal A (2015) Brain tumor segmentation with deep learning. MICCAI Multimodal Brain Tumor Segmentation Challenge (BraTS)
30. Pereira S, Pinto A, Alves V, Silva CA (2016) Brain tumor segmentation using convolutional neural networks in mri images. IEEE Trans ComputImag 35(5):1240–1251
31. Simonyan K, Zisserman A (2014) Very deep convolutional networks for large-scale image recognition. arXiv preprint arXiv:1409.1556
32. Havaei M, Davy A, Warde-Farley D, Biard A, Courville A, Bengio Y, Pal C, Jodoin PM, Larochelle H (2017) Brain tumor segmentation with deep neural networks. Med Imag Anal 35:18–31
33. Chang PD (2016) Fully convolutional deep residual neural networks for brain tumor segmentation. In: International workshop on Brainlesion: Glioma, multiple sclerosis, stroke and traumatic brain injuries, pp. 108–118. Springer
34. Castillo LS, Daza LA, Rivera LC, Arbeláez P (2017) Volumetric multimodality neural network for brain tumor segmentation. In: 13th international conference on medical information processing and analysis, vol. 10572, p. 105720E. International Society for Optics and Photonics
35. He K, Zhang X, Ren S, Sun J (2016) Deep residual learning for image recognition. In: Proceedings of the IEEE conference on computer vision and pattern recognition, pp. 770–778

36. Ghaffari M, Sowmya A, Oliver R (2020) Brain tumour segmentation using cascaded 3d densely-connected u-net.
37. Natarajan, V. Anantha, et al. "Prediction Of Soil Ph From Remote Sensing Data Using Gradient Boosted Regression Analysis." Journal of Pharmaceutical Negative Results (2022): 29-36.
38. Kumar, M. Sunil, et al. "Deep Convolution Neural Network Based solution for Detecting Plant Diseases." Journal of Pharmaceutical Negative Results (2022): 464-471.
39. Prasad, Tvs Gowtham, et al. "Cnn Based Pathway Control To Prevent Covid Spread Using Face Mask And Body Temperature Detection." Journal of Pharmaceutical Negative Results (2022): 1374-1381.1911-1917.
40. Kumar, T. P., & Kumar, M. S. (2021). Optimised Levenshtein centroid cross-layer defence for multi-hop cognitive radio networks. IET Communications, 15(2), 245-256.
41. Natarajan, V. Anantha, et al. "Segmentation of nuclei in histopathology images using fully convolutional deep neural architecture." 2020 International Conference on computing and information technology (ICCIT-1441). IEEE, 2020.
42. P. Sai Kiran. "Power aware virtual machine placement in IaaS cloud using discrete firefly algorithm." Applied Nanoscience (2022): 1-9.
43. Huang G, Liu Z, Van Der Maaten L, Weinberger KQ (2017) Densely connected convolutional networks. In: Proceedings of the IEEE conference on computer vision and pattern recognition, pp. 4700–4708.
44. Bourel P, Gibon D, Coste E. Automatic quality assessment protocol for MRI equipment. Med Phys. 1999;26(12):2693–700.
45. Ahmed, Tashin&Sabab, Noor. (2020). Classification and understanding of cloud structures via satellite images with EfficientUNet. 10.1002/essoar.10507423.1.